ISSN: 0975-766X
CODEN: IJPTFI
Research Article

Available Online through
www.ijptonline.com

PHOTON ANNEALING OF TITANIUM DIOXIDE COATINGS PRODUCED BY MAGNETRON METHOD

Vladimir S. Vaschilin*, Vladimir M. Nartsev, Sergey V. Zaitsev, Dmitriy S. Prokhorencov
Mikhail V. Limarenco, Evgenii I. Evtushenko

Received on 09-08-2016 *Accepted on 05-09-2016*

Abstract

The studies were performed using the methods of spectral ellipsometry, X-ray diffraction and electron microscopy; They revealed the effect of photon annealing on the coating structure made of titanium oxide formed by physical methods (PVD). It was found that during the annealing of coatings deposited at 10 vol. % of O2 in plasma and with the layer of increased Ti content, the greatest changes of structures take place that are presented by the change of film thickness during annealing and grain sintering. In contrast, the photon annealing of coatings deposited at 20 vol. % of O2 in the plasma and without excess Ti atoms, results in a lesser impact on the structure and is accompanied by a smaller change of coating thickness and grain sintering. It was shown that all major changes with the photon annealing of TiOx-coatings deposited by magnetron method occur during the first few minutes of the process, and in the temperature range from 450 °C to 650 °C the rutile structure is developed rapidly.

Keywords: Titanium oxide, magnetron sputtering, photon annealing, ellipsometry, X-ray fluorescent analysis.

Introduction:

The coatings made of titanium oxide (TiOx) are widely used not only in optics to increase the reflection ratio and the synthesis of interference filters [1], but also to create photocatalytic and photovoltaic devices [2], the elements of transparent electronics [3], chemical sensors [4], self-cleaning [5] and some other materials. Moreover, in some cases in order to provide the necessary structure of films based on TiOx it is necessary to perform additional processing. Thus, the structure management capabilities concerning thin film titanium oxides can be significantly enhanced at the combination of physical deposition methods for such coatings with a subsequent heat treatment [6]. Therefore, the studies aimed at the search of relationships between additional processing modes and a structure are of a certain interest for a fine tuning of coating functional properties.

Among different ways of additional effects [7], the photon annealing differs by a rapid uniform heat of a coating because of a short-wave infrared radiation with the simultaneous action of a powerful luminous flux in the visible range. This visible light may influence the phase processes developing in the coatings during annealing. Therefore, the aim of this work is to determine the nature of photon annealing influence on the phase composition and the optical properties of titanium oxide coatings obtained by magnetron method. Materials and methods. TiOx-coatings were prepared by reactive dual magnetron method using the device QVADRA 500 TM (RPC "Alan Praktik") in the argon-oxygen environment (the cleanliness of Ar and O_2 is 99.999% at least). The discharge current made 6 A, the operating pressure was 0.22 Pa, O_2 concentration made 10 and 20 vol. % (for two groups of coatings). Two titanium plates (the proportion of Ti made 99.99 wt. %) were used as targets. The period of titanium dioxide thin film coating made 180 minutes. The substrates were the object plates "MiniMed" with the dimensions 76x26x1 mm and MTO composition (GOST 19808-86). The distance between a target and a substrate was about 10 cm [8]. The annealing of TiOx coatings was performed in the photon vacuum furnace STE RTP 150 (CJSC STA SemiTeq) at different temperature regimes. Before annealing the chamber was dried by the nitrogen stream to -30 °C, the annealing temperature was monitored with a thermocouple. The annealing and coating parameters and the designation of coating samples are shown in Table 1.

Table 1: Annealing modes of TiOx coatings, deposited by magnetron method.

<table>
<tr><th rowspan="2">Series</th><th rowspan="2">O_2 content in plasmaв, vol. %</th><th rowspan="2">Vacuum in a chamber, Pa</th><th rowspan="2">Annealing parameters</th><th colspan="7">Sample number</th></tr>
<tr><th>1</th><th>2</th><th>3</th><th>4</th><th>5</th><th>6</th><th>7</th></tr>
<tr><td rowspan="2">1</td><td rowspan="2">20</td><td rowspan="2">500</td><td>time, min</td><td>-</td><td>1</td><td>2</td><td>4</td><td>8</td><td>16</td><td>32</td></tr>
<tr><td>temperature, °C</td><td>-</td><td colspan="6">500</td></tr>
<tr><td rowspan="2">2</td><td rowspan="2">20</td><td rowspan="2">500</td><td>time, min</td><td>-</td><td colspan="6">4</td></tr>
<tr><td>temperature, °C</td><td>-</td><td>350</td><td>450</td><td>550</td><td>650</td><td>730</td><td>-</td></tr>
<tr><td rowspan="2">3</td><td rowspan="2">10</td><td rowspan="2">900</td><td>time, min</td><td>-</td><td>5</td><td>10</td><td>15</td><td>20</td><td>25</td><td>30</td></tr>
<tr><td>temperature, °C</td><td>-</td><td colspan="6">500</td></tr>
</table>

The optical properties were studied using the modulation spectral ellipsometer "Uvisel 2" (Horiba Jobin Yvon). Spectral measurement range made 192-2047 nm with the scanning step of 7 nm. As the substrate is a thin one, the incidence angle made 60° to avoid the getting of beams into the ellipsometer detector reflected from the lower boundary "substrate-air". The selection of coating layer structure model, the calculation of thicknesses and layer optical properties was carried out under the program "DeltaPsi2" (Horiba Jobin Yvon). The adequacy of model coatings was estimated by the sum of the squared deviations between the experimental and calculated data (parameter $[xi]^2$)

$$\chi^2 = \sum_{i=1}^{N}\left[\left(\Psi_{\text{mod,i}} - \Psi_{\text{exp,i}}\right)^2 / \sigma^2_{\text{exp},\psi i} + \left(\Delta_{\text{mod,i}} - \Delta_{\text{exp,i}}\right)^2 / \sigma^2_{\text{exp},\Delta i}\right] / (NM - K), \qquad (1)$$

where N – the number of data points in the spectrum (N = 1856), M - the number of spectra used for calculation (M = 2), K - the number of adjustable parameters (from 17 to 24 depending on the number of layers in the coating model and the number of coefficients in the equations of dependences concerning the refraction and absorption indices of these layers), $[PSI]_{mod,i}$, $[DELTA]_{mod,i}$, $[PSI]_{exp,i}$, $[DELTA]_{exp,i}$ – model (calculated) and experimental values of the ellipsometric angles [PSI] and [DELTA], respectively, $[sigma]_{exp, [PSI]i}$ and $[sigma]_{exp, [DELTA]i}$ – standard deviations during angle measurement [PSI] and [DELTA] respectively ($\sigma_{exp, [PSI]i}$ и $\sigma_{exp, [DELTA]i}$ ~ 0,01). For all studied samples the values $[xi]^2$ did not exceed 10, and the refractive index and absorption coefficient values were calculated for a wavelength of 600 nm. The crystal structure and the preferred orientation of grains for thin TiOx coatings were studied by X-ray diffraction ARL X`TRA (Thermo Techno) in the angle range 2[theta] from 20 degrees to 70 degrees with the increment of 0.02°. In order to identify the phases and index peaks JCPDF file was used.

Surface morphology and coating fracture patterns were investigated using a scanning electron microscope of high resolution TESCAN MRA 3 LMU.

Main part;

The ellipsometric measurements show that clear coatings obtained at 20 vol. % of O2, have a two-layer structure, and the translucent coatings deposited at 10 vol. % of O2 are characterized by a three-layer structure. Fig. 1 shows typical spectra of ellipsometric angles obtained from the coatings for specified deposition conditions.

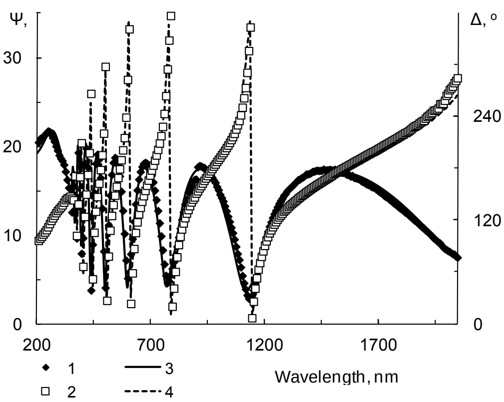

а

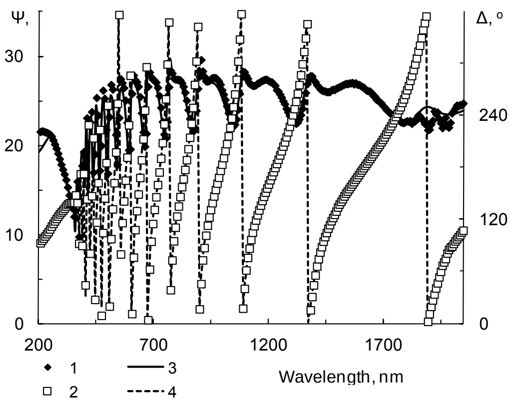

б

Fig. 1. The spectral dependences of measured (1, 2) and model (3, 4) ellipsometric angles ([PSI] and [DELTA]) for the samples deposited at 20 vol. % of O2 (a) and 10 vol. % of O2 (b) 1, 3 - [PSI], 2, 4 - [DELTA].

In the first case, they may identify only the main and the roughened layer (the angle [PSI] varies within 0-20^o range), in the second case there is an additional contact layer, which has a high optical absorption, probably because of the high content of Ti atoms ([PSI] angle varies in the range of 20-30^{o}). Photon annealing for the third series of samples reduces the coating thickness by almost 12% mainly due to the sealing of the base layer, the increase of contact layer thickness and the disappearance of the rough layer, according to ellipsometric data (Fig. 2).

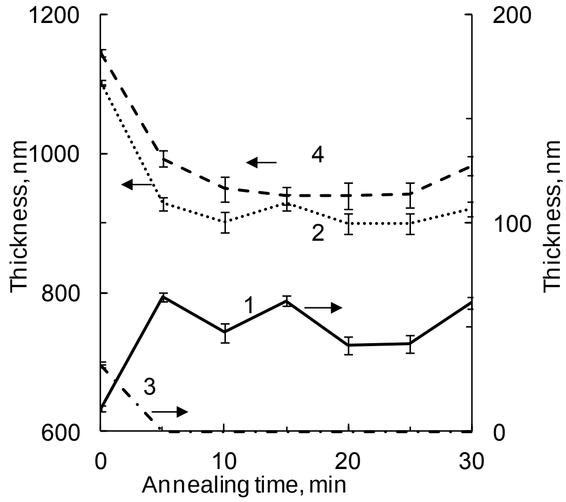

Fig. 2. Dependencies on the duration of annealing for the thickness of coating layers (the third series of samples): 1 - contact layer, 2 - base layer 3 - rough layer 4 - coating thickness.

The reason of the base layer sealing may be represented by sintering which reduces porosity, and crystallization (or recrystallization) accompanied by the release of the densest phase, that is rutile. In both cases the refractive index of the base layer will be increased, as evidenced by Fig. 3.

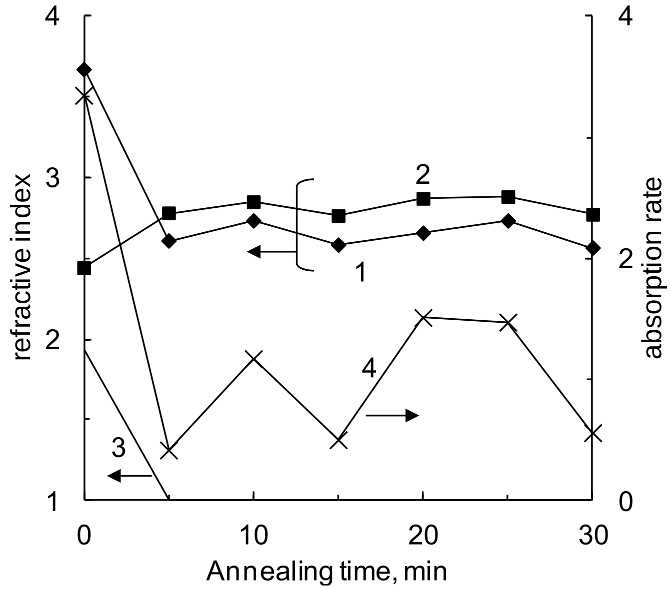

Fig. 3. Dependencies of refractive (1-3) and absorption (4) index of layers on the annealing period; 1, 4 - contact layer, 2 - base layer, 3 - roughened layer.

The growth of the contact layer thickness is uniquely associated with the diffusion of redundant Ti atoms and their partial oxidation by oxygen adsorbed in the pores, evidenced by the decrease of refraction and absorption values during the first 5 minutes of annealing (Fig. 3, curves 1 and 4). According to ellipsometry, the disappearance of a rough layer looks strange as the annealed samples (Fig. 4 b, d, f, h, j, l, n) clearly demonstrate non-uniform roughness, which can't be calculated in ellipsometric method (due to poor development of light propagation model in such systems). Two sections may be revealed conditionally on the fracture patterns of annealed coatings as compared to the initial sample: one, contacting with a substrate, has the structure characteristic of the sintered materials, other has a columnar grain structure of the original coating, but somewhat sparse one.

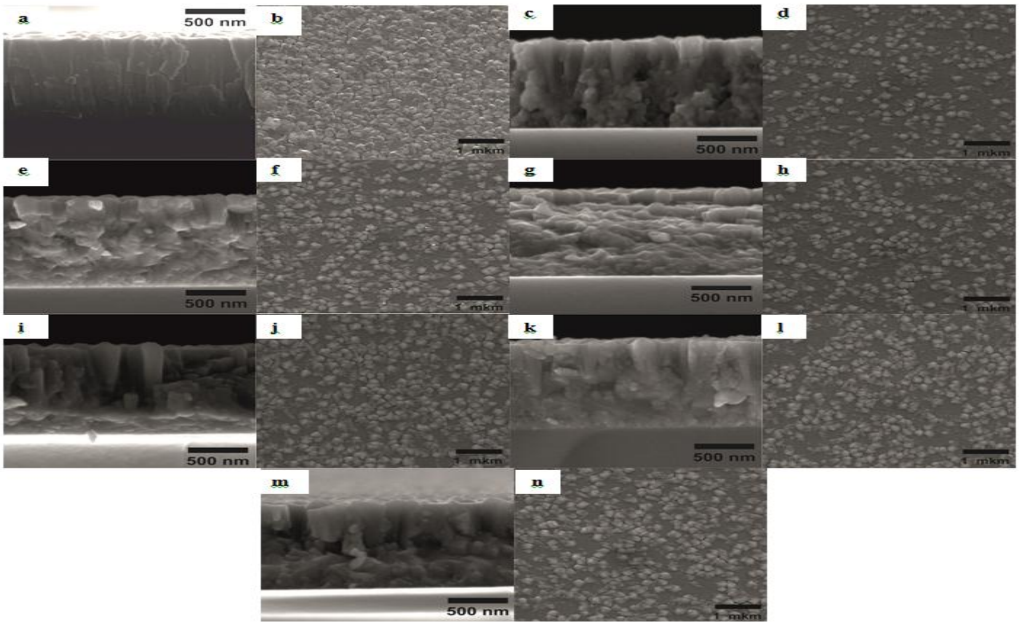

Fig. 4. The fracture patterns (a, c, e, g, i, k, m) and the surface (b, d, f, h, j, l, n) of TiO_x coatings depending on the time of photon annealing for the third series of samples: a, b – without annealing; c, d –5 min; e, f –10 min; g, h –15 min; i, j – 20 min; k, l – 25 min; m, n – 30 min.

If we compare the dependencies of coating thickness obtained according to ellipsometry and electron microscopy data (Fig. 5), the mirror symmetry of curves, which indicates correlation values can be noted besides the significant differences.

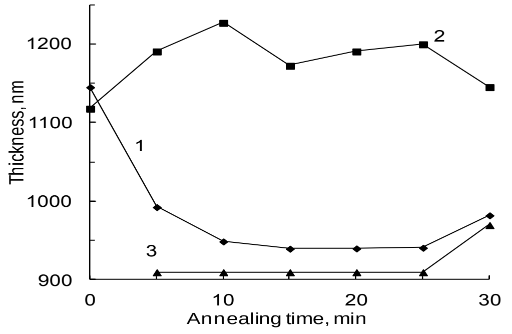

Fig. 5. The dependencies of coating thickness on the annealing time: 1 - coating thickness according to ellipsometry data, 2 - coating thickness according to electron microscopy, 3 - the thickness of the sintered portion according to microscopy data.

The similarity of the curves 1 and 3 on the Fig. 5 points to the identity of the sintered area, observed by microscopy and the base layer at the ellipsometric modeling of the coverage.

The phase composition, which is presented by the amorphous component for the initial coating and a small amount of anatase, also undergoes major changes during the first 5 minutes of photon annealing (Fig. 6)

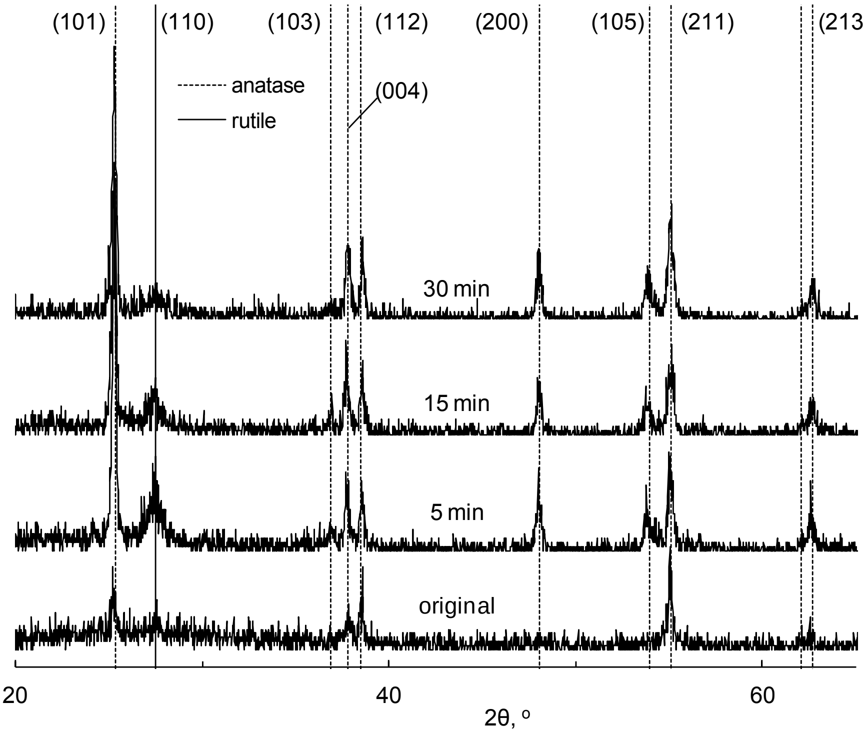

Fig. 6. Diffraction patterns of coatings depending on the duration of photon annealing for the third series of samples.

In particular, there is the growth of anatase grains observed in the initial coating along the trend (101), (004), (211), (213), and crystallization takes place, probably from the amorphous component, the grains of anatase and other orientations (giving the following peaks: (200) and (105)). Also a number of small grains of rutile is developed. At that the development of its crystallization is prevented probably by the available anatase grains. The continuous annealing leads to a relative decrease of rutile peak height (110), that can be related to the diffusion in the coating of substrate components, in particular with Na2O, and the formation of titanates.

According to the obtained data, we may conclude that all major changes during the photon annealing of TiOx-coatings deposited by magnetron method take place during the first few minutes of the process. These changes are reduced the sintering of areas containing a large number of pores, the grains with an active (defect) structure, as well as the grains, polished by high-index planes. Sintered areas are recrystallized probably, and the grains, which were faceted by low-energy planes in the original coating, continue to grow. The diagram (Figure 7) is presented below showing these structural changes.

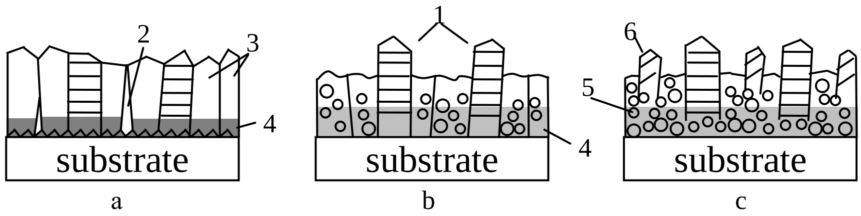

Fig. 7. Approximate scheme of the structure change in terms of photon annealing at 500 °C for TiO_x coatings with an excessive content of Ti in the contact layer: a - original coating, b - short annealing, c - prolonged annealing, 1 - grain, polished by low-energy facets, 2 - pore, 3 - defective grains, 4 - the layer with the excess of Ti, 5 - sintered areas 6 - the grains grown from sintered portions.

In order to enhance the ideas about the impact principles of photon annealing on the structure of coatings the samples of the first series were studied in which there was no contact layer with a high concentration of titanium.

The coatings of the first series also become thinner, but at 4% during the first minutes of photon annealing (Fig. 8).

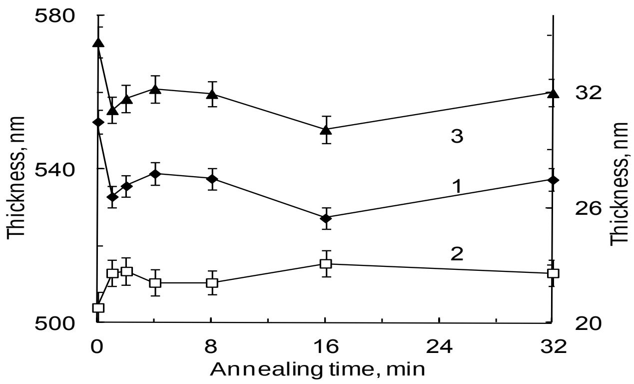

Fig. 8. The dependencies on the duration of the coating layer thickness annealing (the first series of samples): 1 - base layer, 2 - rough layer, 3 - coating thickness.

As compared to the initial sample of the third series, the original coating of the first series contains less anatase and more amorphous components, orientation grains (200) and (105), as well as a larger amount of rutile nuclei (Fig. 9).

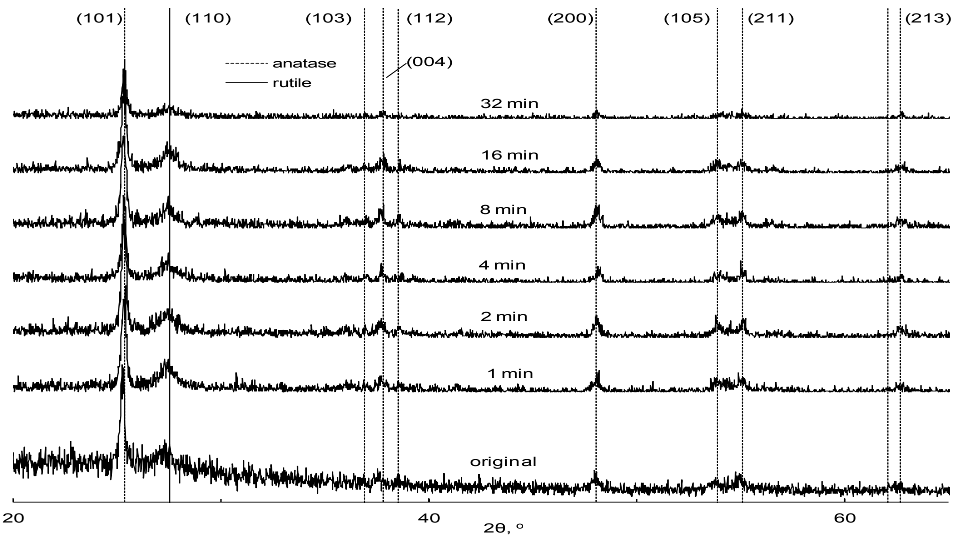

Fig. 9. Diffraction patterns of coatings depending on the duration of photon annealing for the first series of samples.

Primarily this difference is conditioned by different coating thicknesses and oxygen concentrations during synthesis. The fact is that during the magnetron sputtering the thickness increase leads to the accumulation of energy by coating, which is used to overcome the activation barriers of crystallization. The increase of oxygen concentration increases the energy of deposited atoms which results in its surface mobility increase and the ability to develop the embryos of grains with different orientations. Therefore, the first series coatings are crystallized to a lesser extent (the peak height is less, and the peak width is greater) and they have not only the anatase embryos of all orientations, but also rutile embryos. Photon annealing, as for the abovementioned case, increases the crystallinity degree of coating during the first minutes and reduces the degree of coating crystallinity at long annealing. At that the relative volume of anatase grains, which will be assumed as the proportional one of the anatase peak height (101) to the sum of peak heights (110), rutile and (101) anatase, correlates with the height of the roughness layer, at least with the annealing periods not exceeding 16 minutes (fig. 10).

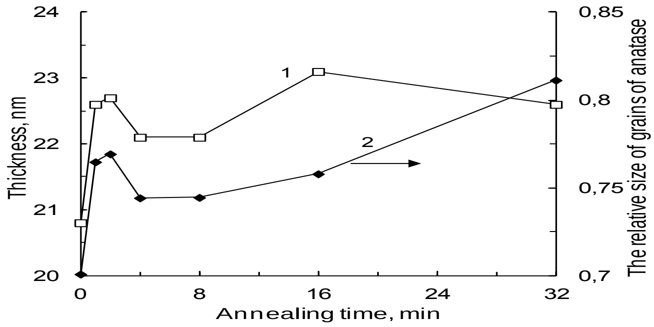

Fig. 10. The dependencies on the period of annealing concerning the relative volume of anatase grains (1) and the height of the roughness layer (2).

Consequently, the development of roughness in the first series of surfaces is conditioned by the growth of anatase orientation grains (101). It should be noted that the annealing in the range of 1-8 min results in a similar change tendency of the grain size (Fig. 11a, c, e, g, i, k, m) [9].

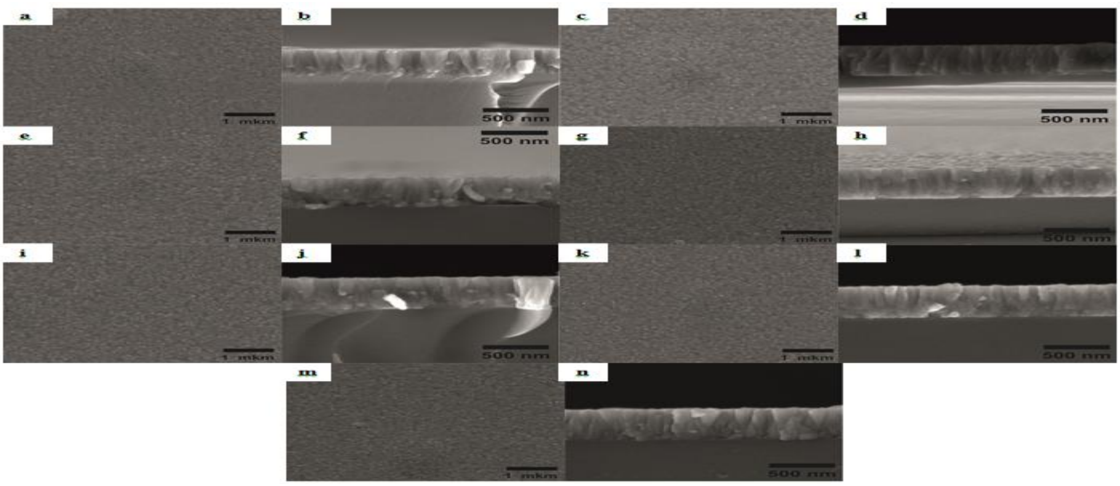

Fig. 11. The surface (a, c, e, g, i, k, m) and fracture patterns (b, d, f, h, j, l, n) of TiO_x coatings depending on the time of photon annealing for the first series of samples: a, b - without annealing; c, d - 1 min; e, f - 2 min; g, h - 4 min; i, j - 8 min; k, l - 16 min; m, n - 32 min.

That is, for the first minute the average grain diameter increases from 75 to 100 nm, during the second minute the diameter remains practically unchanged, during the fourth minute the diameter is reduced to 80 nm and then remains substantially constant. Since there are no significant changes of structure concerning the thickness of coatings (Fig. 11 b, d, f, h, j, l, n), the excess of Ti in the contact layer of the third series samples plays the role of a sintering activator. A small increase of the refractive index within the basic layer during the beginning of annealing (Fig. 12, curve 1 and 2) is associated with the crystallization of anatase and particularly rutile, which has a higher refractive index.

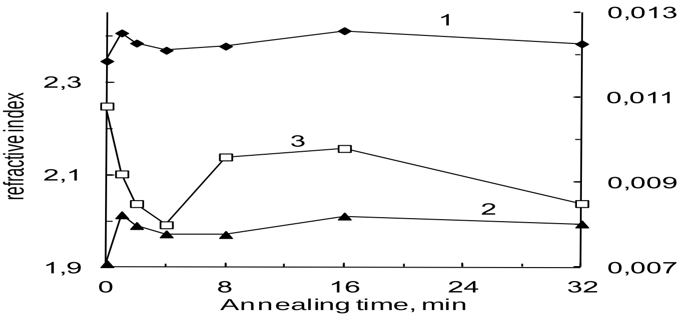

Fig. 12. The dependence of the refraction (1.2) and absorption (3) index in coating layers on the annealing duration: 1, 3 - base layer, 2 - roughened layer.

The relatively low values of the absorption coefficient for the base layer are caused not by excess Ti atoms, but by the division limits between the grains that scatter a beam during ellipsometric measurements. Accordingly, during the first 4 minutes the number of such boundaries decreases due to the partial sintering and crystallization. In the range of 8-16 minutes the grains with the orientation (112) and (004) appear, which increase the number of boundaries that scatter light. Then the recrystallization process starts apparently complicated by the diffusion of substrate components, leading again to the reduction of the number of boundaries. In the case of the first series of samples the coating thicknesses obtained by various methods cooperate with each other better undoubtedly (Fig. 13) than the third series of samples.

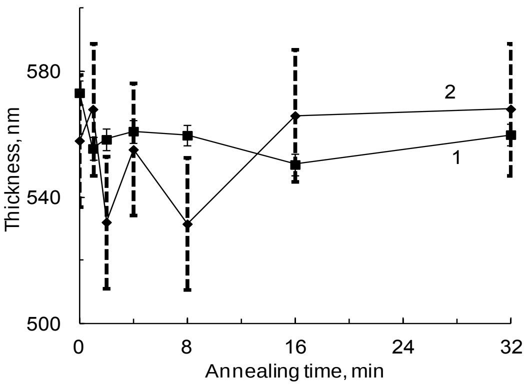

Fig. 13. The comparison of TiOx coating thickness obtained by ellipsometry (1) and microscopy (2) for the first series of samples.

This situation is explained by a much lower concentration of the sintered areas between grains. For example, on Fig. 4 «d» the surface is presented by relatively few crystalline grains, while the surfaces of all samples are filled quite densely for Fig. 11.

While the variation of the annealing time at 500 °C gives a very sharp change of the coating structure at the process beginning the samples annealed within the same time but at different temperatures (the second series) were produced and studied. The temperature of photon annealing increase to 450 °C leads to a gradual reduction of the coating thickness at the simultaneous smooth increase in the refractive index (Fig. 14), which is associated with the sintering processes and porosity reduction.

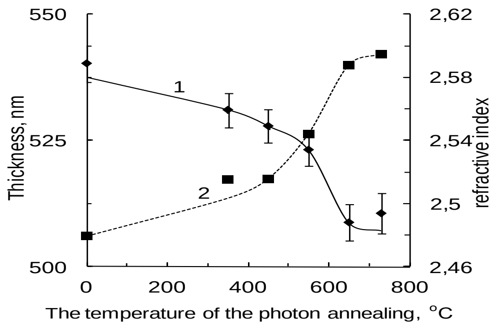

Fig. 14. Photon annealing temperature dependence on the thickness of coating (1) and the refraction index of the base layer (2) defined by ellipsometric method.

The greatest changes in coating structure occur in the range of 450-650 °C, which are accompanied by an abrupt decrease of thickness and the refractive index increase, the cause of which is the rutile crystallization, as anatase refractive index ~ 2.4 and rutile refractive index ~ 2.6. The concentration of rutile phase increase is confirmed by X-ray diffraction method (Fig. 15 and 16) [10].

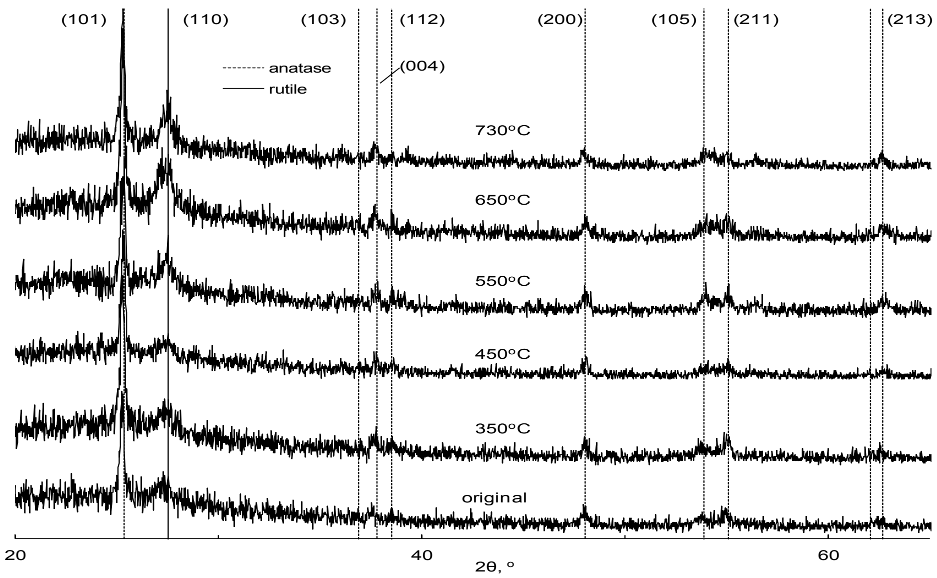

Fig. 15. Diffraction patterns of coatings depending on the duration of photon annealing for the first series of samples.

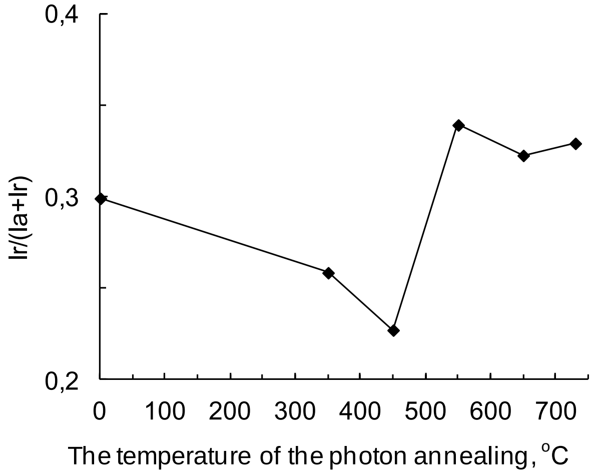

Fig. 16. The dependence of the peak intensity ratio (110) to the sum of anatase (101) and rutile (110) $I_r/(I_a+I_r)$ on temperature.

According to X-ray diffraction anatase is crystallized up to 450 °C, then rutile develops more intensively within the range of 450-650 °C, but the structure is still sufficiently porous one at this temperature so the refractive index does not correspond to rutile. Only after the sealing of structure at 650 °C the base layer attains the refractive index of bulk rutile.

The change of thickness and a phase state is consistent with the grain size change observed on coating surface by electron microscopy (Fig. 17).

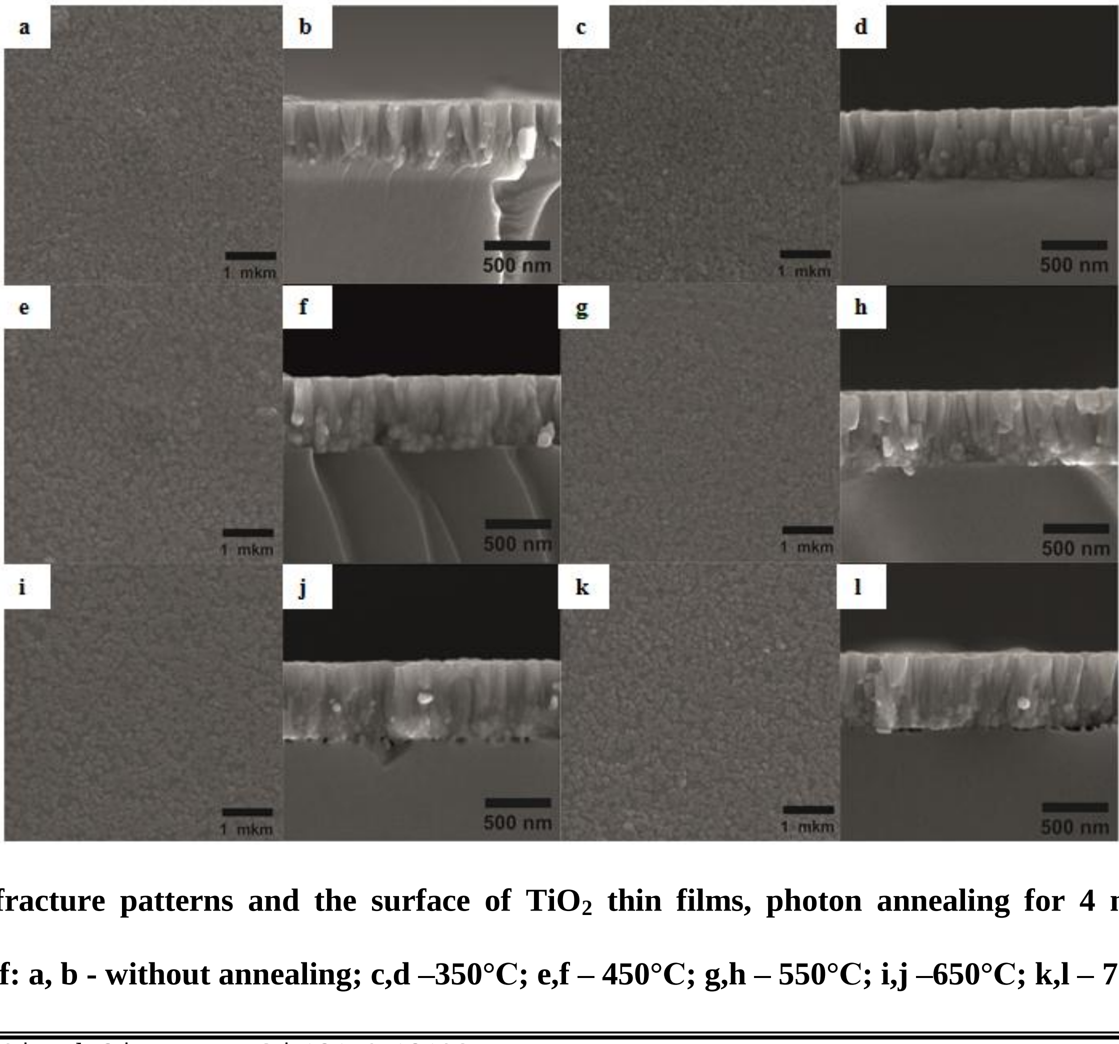

Fig. 17. The fracture patterns and the surface of TiO_2 thin films, photon annealing for 4 minutes at the temperature of: a, b - without annealing; c,d –350°C; e,f – 450°C; g,h – 550°C; i,j –650°C; k,l – 730°C.

Thus, the grain size is increased from 75 to 100 nm with the temperature increase up to 450 °C. At 550 °C the grains are increased sharply to 120 nm and the sintering areas become noticeable. The images of coating surfaces are similar for 650 ^{o}C and 730 ^{o}C, while the grains have almost the same size, and the sintering areas occupy the maximum area for this series of samples.

Similarly to the first series of samples (Fig. 13), the dependencies of coating thickness, obtained by different methods are absolutely symmetrical ones for the second series of samples (Fig. 18) due to the development of relatively large areas with the sintered structure and the growth of individual grains.

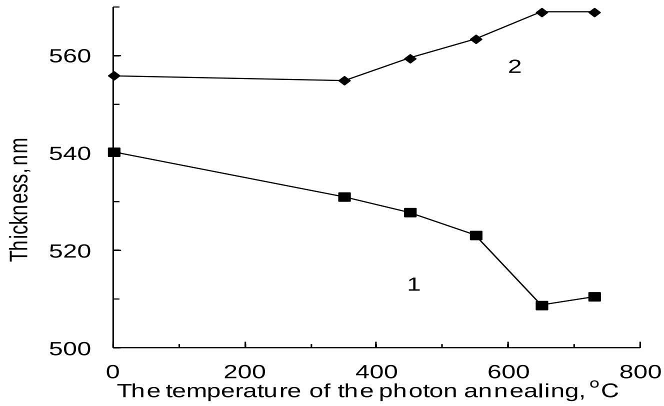

Fig. 18. The dependencies of coating thickness on the annealing temperature: 1 - coating thickness according to ellipsometry data, 2 - coating thickness according to electron microscopy data.

Chipped initial sample and the samples annealed in the range of 450 C differ little from each other, whereas the layer is observed in the area of a surface and a substrate contact, characteristic for the sintered material within the temperatures of 550-650 ^{o}C (Fig. 17 g, h, i, k).

Summary: In this paper, we performed the studied by the methods of spectral ellipsometry, X-ray diffraction and electron microscopy; They revealed the effect of photon annealing on the coating structure made of titanium oxides developed by physical methods (PVD).

Conclusions: It was found out that the structure of formed coatings based on titanium dioxide, depends on the nature of photon annealing and on the conditions of magnetron titanium sedimentation. It is found that at the annealing of coatings deposited at 10 vol. % of O2 in plasma with an oxide layer with a high content of Ti, the greatest changes of the structure take place which are represented by the change of coating thickness within almost 12% during the annealing (mainly due to the sealing of the base layer according to ellipsometry data) and the sintering of grains, the photonic annealing of coatings deposited at 20 vol. % of O2 in the plasma containing titanium dioxide close to stoichiometric one, results in a smaller impact on the structure and is also accompanied by the sintering of grains, but with a lower variation of coating thickness about 4%.

According to performed studies of photon annealing at 450 °C in the thin films of TiOx coating anatase is crystallized, then rutile is developed intensively in the range of 450-650 ^{o}C.

You may also conclude that all major changes at the photon annealing of TiOx-coatings deposited by magnetron method occur during the first minutes of the process. These changes are reduced to the sintering of areas containing a large number of pores, the grains with an active (defect) structure, as well as the grains, polished high-index planes. The sintered areas are recrystallized during further annealing, and the grains, which were faceted by low-energy planes in the original coating, continue to grow.

The work was supported by RFBR grant 14-41-08064 r_ofi_m and the Strategic Development Program of BSTU named after V.G. Shukhov during 2012-2016.

References

1. Pugachevsky, M.A., 2012. Morphological and phase changes of ablated TiO2 particles during thermal annealing. TPJ letters, vol. 38, issue № 7: 56-63.
2. Ko, K.H., Y.C. Lee and Y.J. Jung, 2005. Enhanced efficiency of dye-sensitized TiO_2 solar cells (DSSC) by doping of metal ions, Journal of Colloid Interface, 283: 482–487.
3. Zainullina, V.M., V.P. Zhukov, V.N. Krasilnikov, M.Y. Yanchenko, L.Y. Buldakova and E.V. Polyakov, 2010. Electronic structure, optical and photocatalytic properties of anatase doped by vanadium and carbon. Solid State Physics, Volume 52, no. 2: 253-261.
4. Karunagaran, B., P. Uthirakumar, S.J. Chung, S. Velumani and E.K. Suh, 2007. TiO2 thin film gas sensor for monitoring ammoni. Mater. Characterization. 58: 680-684.
5. Kitano, M., M. Matsuoka, M. Ueshima and M. Anpo, 2007. Recent developments in titanium oxide-based photocatalysts. Appl. Catal. A, 325(1): 1-14.
6. Nartsev, V.M., D.S. Prohorenkov, N.V. Osipenko, S.V. Zaitsev and E.I. Yevtushenko, 2012. The study of TiOx coating properties formed using the vacuum-plasma technologies. Fundamental Research, 11: 1195-2001.
7. Kobl, P., M. Huppertz and D. Mergel, 1994. Nucleation and growth in TiO_2 films prepared by sputtering and evaporation. Thin solid films: 72-79.
8. Zaitsev, S.V., V.S. Vaschilin, D.S. Prohorenkov, V.M. Nartsev and E.I. Yevtushenko, 2015. The structure of the thin films made of tin dioxide generated by dual magnetron sputtering. Bulletin of named after V.G. Shukhov, 5: 228-231.

9. Zapata-Torres, M., E. Hernández-Rodríguez, R. Mis-Fernandez, M. Meléndez-Lira, O. Calzadilla Amaya, D. Bahena, V. Rejon and J.L. Peña, 2015. Visible and infrared photocatalytic activity of TiO_x thin films prepared by reactive sputtering. Materials Science in Semiconductor Processing, 40: 720-726.

10. Arnaud Cacucci, Olivier Heintz, Ioannis Tsiaoussis, Ludovic Avril, Valérie Potin, Luc Imhoff, Nicolas Martin, 2014. Flash annealing influence on structural and electrical properties of TiO_2/TiO/Ti periodic multilayers. Thin Solid Films, 553: 47-51.

Corresponding Author:

Vladimir S. Vaschilin*,